PAPER

Check for updates

Saturated adsorption of lidocaine and coal tar dyes onto porous polytetrafluoroethylene†

Kengo Mitsuya, Satoru Goto, [ID] * Yuta Otsuka, Yayoi Kawano and Takehisa Hanawa [ID]

Polytetrafluoroethylene (PTFE) has excellent physical properties and has been used in a wide range of applications in various fields. Adsorption research on PTFE is essential as primary research for the further application of PTFE. We attempted to adsorb coal tar dyes and model drugs such as lidocaine onto PTFE as a guideline to search for medicines that adsorb onto PTFE. Saturation curves were obtained after analyzing the adsorption of coal tar dyes on PTFE using the Hanes–Woolf plot. In addition, we collected multiple cases of ATR-FTIR spectral changes and/or retention depending on TPM derivatives and other adsorbates. Lidocaine matched some coal tar dye for the apparent spectral changes between the adsorbed molecules and its crystalline powder. The apparent spectral changes are blue-shifted, suggesting a hydrophobic interaction between the dyes/lidocaine and porous PTFE. This work provides a promising strategy for further application of PTFE.

Introduction

Porous polymeric membranes have been researched for many potential applications, including catalytic reaction,[1] filtration,[2] and energy storage.[3,4] These membranes have been manufactured using mechanical stretching,[5] spinning,[6] and poreforming agent methods.[7] Polyethylene, polysulfone, poly(-vinylidene fluoride), polydimethylsiloxane, polypropylene, polyimide, and polytetrafluoroethylene (PTFE) are common types of porous polymeric membranes. Among them, PTFE is attracting attention because it is biologically inert, noncarcinogenic, and stable in the presence of infection. Because of these properties, PTFE is used as an artificial organ, such as an excellent synthetic fascial option for major abdominal wall defects or incisional hernias.[8]

PTFE has many other benefits including excellent chemical resistance, thermal stability, and high mechanical strength. Because of its wide practical application potential, PTFE is used not only in the medical field[8,9] but also in pharmaceutical industries,[10] petrochemical,[11] semiconductor,[12] and chemical processing.[13] However, the adsorption of pharmaceutical molecules onto PTFE has not yet been reported. Because of the strong C–F bond in PTFE, there is no interaction between PTFE and the drug due to hydrogen bonds, suggesting no possibility of adsorption of pharmaceuticals onto PTFE.[14,15] While the biologically inert surface indicates no interaction with the drug, many proteins, such as insulin and immunoglobulin G, have

already been reported to adsorb onto PTFE *via* hydrophobic interaction.[16–18] Recently, the adsorption of pharmaceuticals onto solid media has been studied, and it has been applied in various industries and medical treatments. For example, in industry, the application of sonication to improve the properties of activated carbon has been developed to produce a solid adsorbent capable of removing ibuprofen and ketoprofen from aqueous media.[19] In the medical field, bentonite has been reported to be used for the sorption of thiabendazole to create new drug delivery systems and controlled release systems.[20] As PTFE is nontoxic to living organisms, if the adsorption of lidocaine (LDC) to PTFE is possible, we considered that it could be used to remove excessive LDC intake during dental treatment.

LDC is one of the most common drugs used in dentistry[21] and has been reported to be used with dexmedetomidine in dental procedures.[22] In our previous studies, LDC changed the solubility of poorly soluble drugs. Adding LDC to indomethacin (IND) decreases the melting temperature and fusion enthalpy to form a sustainable amorphous structure.[23] Local anesthetics were attempted to partner the co-amorphization with IND. The apparent octanol/water partition coefficients of the mixtures showed an excellent relationship with intrinsic hydrophobicity and molecular structural flexibility.[24] The addition of LDC and procaine, which have low hydrophobicities, provide IND with an apparent increase in hydrophobicity, while simultaneously increasing the apparent aqueous solubility.[25] This indicates that the intermolecular interaction between LDC and IND is not as simple as forming a hydrophilic/hydrophobic complex. Ibuprofen, which has low molecular weight and hydrophilicity, loses its aqueous solubility when LDC is added and

forms an ionic liquid layer separated under an aqueous solution.[26] However, a similar insoluble LDC and IND mixture layer did not form. From the van't Hoff plot for solubility of acidic and basic drugs and their mixture, we found that the dissolution enthalpy of the NSAIDs changed from positive to negative, induced by mixing with local anesthetics.[27] However, LDC is colorless, and its adsorption is challenging to evaluate qualitatively.

Organic dyes are helpful for evaluating adsorption onto PTFE. In the dye-related industry, water pollution by organic dyes is regarded as a problem. To solve this problem, the adsorption of organic dyes onto a solid medium has been investigated for a long period. For example, polydopamine microspheres have been investigated as highly efficient selective adsorbents for some cationic dyes.[28] In addition, organic dyes are used as tracers because they have an absorption band in the visible region. For example, organic dyes have been used to analyze various complicated flow situations for a flow visualization technique called the photochromic dye method.[29] More specifically, organic dyes are often used in the evaluation of adsorbents. Adsorption can be visualized, and the best way to achieve this is to use organic dyes to investigate the adsorption conditions on PTFE. For many organic dyes, we used coal tar dyes.

In this study, as a primary research for further application of PTFE membranes, we realized coal tar dyes/LDC adsorption onto a porous PTFE membrane. Adsorption of organic dyes on PTFE may be used to remove organic dyes, which are toxic substances in the environment. Furthermore, PTFE could remove an overdose of LDC, a local anesthetic used in dentistry.

Materials and methods

Materials

Remarks on the intact PTFE membrane, porous PTFE membrane, filter paper, nitrocellulose filter (NCF), polycarbonate membrane (PCM), and JHWP04700 are listed in Table 1. The contents of a conventional material transfer agreement restricted the disclosure of information on iPTFE and pPTFE.

Reagents: amide black 10 B (AB), bromothymol blue (BTB), Coomassie brilliant blue G250 (CBB), fluorescein (FL), fuchsine (FC), LDC, malachite green oxalate (MG), methylene blue (MB), methyl orange (MO), rhodamine 6G (R6G), Sudan III (SD) were purchased from Sigma-Aldrich (St. Louis, MO, USA), and Wako Pure Chemical Industries (Osaka, Japan). All other reagents were of the highest commercially available grade.

Adsorption of dyes/lidocaine on the intact PTFE, porous PTFE, JHWP04700 (hydrophilic PTFE), nitrocellulose, polycarbonate, and filter paper membranes

Aqueous solution-stained membranes were prepared as follows: each membrane was fragmented to a 1 cm × 1 cm square and soaked in an aqueous solution containing 1 mg mL^{-1} of sample dye in 0.2 mmol L^{-1} of phosphate buffer (pH 6.8). The solution was shaken at 500 rpm for 24 h at 25 °C, and the stained membrane was obtained from the solution and air-dried at ambient temperature for 24 h.

The evaporative dried membranes were prepared as follows. First, the prescribed membrane fragment was soaked in acetone solution of sample dye at the concentration of 0.5 mg mL^{-1}; then, it was air-dried until the solvent volatilized. Subsequently, the stained membrane was washed with ultrapure water to exhaust the colored waste and air-dried for 24 h.

Appropriate-solvent-stained membranes were prepared, and the solvent was experimentally selected from water, ethanol, chloroform, acetone, pyridine, toluene, and cyclohexane. The prescribed membrane fragment was soaked in 2 mmol L^{-1} of dye solution with the most appropriate solvent for 30 min. Subsequently, the stained membrane was dried by inserting bundled laboratory cleaning tissue paper (KimWipes®, Nippon Paper Crecia Co., Ltd., Tokyo, Japan) for 24 h.

The adsorption of LDC onto the porous PTFE membrane was similar to that of the evaporative dried membranes. First, the porous PTFE membrane fragment was soaked in the 2-propanol solution of LDC at the concentration of 0.2 mol L^{-1}, and air-dried until the solvent volatilized. Subsequently, the adsorbed membrane was washed with ultrapure water and air-dried for 24 h.

A camera was used to capture photos of the stained membranes, pointed perpendicular to the membrane surface plane under natural light.

Differential scanning calorimetry

Differential scanning calorimetry (DSC) measurements were performed using 3 mg of analyte (i.e., neat powder or stained membrane) in a closed aluminum pan using a DSC-60 Plus (Shimadzu, Co., Kyoto, Japan) instrument. The analyte was heated from 298 to 368 K at the rate of 5 K min^{-1} under a nitrogen gas flow with velocity of 30 mL min^{-1}.

Attenuated total reflectance-Fourier transform infrared spectroscopy

Fourier transform infrared (FT-IR) spectra of the samples were obtained using a Frontier FT-IR spectrometer (PerkinElmer Co., Ltd., Waltham, MA, USA) via attenuated total reflection (ATR)

Table 1 Used membranes, their materials, and remarks

Membrane	Material	Remarks
iPTFE	Intact PTFE	Hydrophobic water-repellent
pPTFE	Porous PTFE	Hydrophobic water-repellent polar (ϕ 0.6 μm)
NCF	Nitrocellulose	Hydrophilic polar (pore size ϕ 0.45 μm)
PCM	Polycarbonate, $(-O-X-O-CO-)_n$	Hydrophobic polar (ϕ 0.2 μm)
JHWP04700	PTFE, $(-CF_2CF_2-)_n$	Polar (ϕ 0.2 μm)

under spectral resolution of 1 cm^{-1}. The spectra were observed using a single bounce diamond anvil ATR cell.

The ATR-FTIR spectra of the dyes adsorbed onto the porous PTFE membranes were obtained after subtracting the background (porous PTFE) from the sample (stained porous PTFE) spectra.

Reflective absorbance with the integrating spherical spectrophotometer

Evaporative dried membranes and appropriate-solvent-stained membranes were molded into 5 mm × 5 mm squares using a cutter knife. The molded membrane was set onto the operating stage of the spectrophotometer (V-750, Jasco Co., Tokyo, Japan). The visible light absorption spectrum was scanned at wavelengths of 380–800 nm at intervals of 1 nm. A complete reflective reference (instrumental standardized white plate) was used as the standard. By measuring the corresponding non-stained membrane as a baseline, the comparative absorbance of the stained membranes for the sample dyes was recorded.[30]

Scanning electron microscopy of membranes

The samples were placed on a sample holder using double-sided adhesive tape. Upon adhesion, the samples were coated with platinum in a high-vacuum evaporator (JFC-1600, JEOL Ltd., Tokyo, Japan) and imaged *via* scanning electron microscopy (SEM, JSM-6060LA; JEOL Ltd., Tokyo, Japan).

Results and discussion

Screening of chemicals sustainably capable of staining porous PTFE

The DSC thermogram of LDC adsorbed onto the porous PTFE membrane and the ATR-FTIR spectra are shown in Fig. 1. We observed an endothermal signal at a temperature lower than the melting point of the crystalline LDC powder on a DSC thermogram (Fig. 1A). The apparent change between the ATR-FTIR spectra of the LDC crystalline powder and the LDC adsorbed onto the porous PTFE membrane is negligible, and the changes

at wavenumbers of 1198 and 1148 cm^{-1} are related to the PTFE-derived absorption (Fig. 1B). However, these results do not confirm whether LDC adsorbed onto the porous PTFE membrane was an intact crystal. These observations indicate that verification of the adsorption of chemicals on the examined membranes is required in advance. Therefore, we are interested in visible dyes as traceable and comparatively determinable adsorbates.

Initially, hydrophilic or hydrophobic dyes, dissolved in inorganic phosphate/NaOH buffer, failed to adsorb on the intact PTFE membrane and porous PTFE membrane under the conditions available for their adsorption on the JHWP04700 membrane, NCF, and PCM. The NCF, PCM, and filter paper exhibit typical properties. NCF is a hydrophilic membrane with a smooth surface, PCM is a hydrophobic membrane with a smooth surface, and filter paper is a hydrophilic membrane with a rough surface and steric hindrance. In addition, a comparative experiment was conducted using a commercially available PTFE membrane, JHWP04700. Compared with AB, MB, and SF, a slightly higher retention of CBB and MG on the porous PTFE membrane was observed (ESI Fig. S1†). The selected dyes were AB as a hydrophilic diazo dye, MB as a basic thiazine dye, SF as a lipophilic cationic dye, and CBB and MG as triphenylmethane (TPM) derivative dyes. We focused on the propeller structures of TPM dyes. Subsequently, evaporative dried membranes were prepared and soaked in analogous dyes (BTB, FC, FL, and R6G) dissolved in acetone. These dyes are
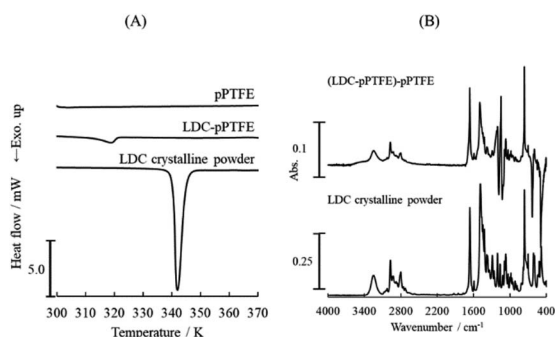

Fig. 1 (A) DSC thermogram and (B) ATR-FTIR spectra of lidocaine (LDC) adsorbed onto the porous PTFE membrane. LDC adsorbed onto porous PTFE membrane was prepared as described in the Materials and methods section. The difference spectrum, named (LDC-PTFE)-PTFE, was obtained after subtracting the porous PTFE from the LDC-adsorbed porous PTFE.
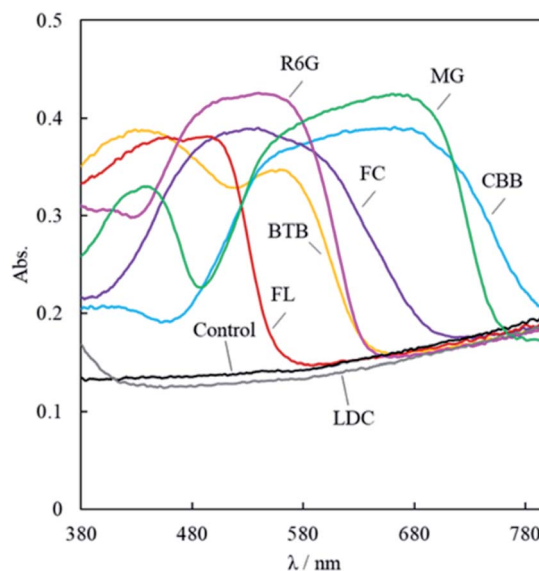

Fig. 2 Reflective spectra of TPM derivatives staining the porous PTFE membranes and the LDC-adsorbed porous PTFE measured using the integrating spherical spectrophotometer. The porous PTFE membranes were excised as 5 mm × 5 mm, and then soaked in acetone solution of the TPM derivatives. The evaporative dried membranes were prepared as described in the Materials and Methods section. BTB, CBB, FC, FL, MG, R6G, and LDC are abbreviations for bromothymol blue, Coomassie brilliant blue R-250, fuchsine, fluorescein, malachite green oxalate, rhodamine 6G, and lidocaine, respectively. Control represents the reflective spectrum of a non-stained membrane.
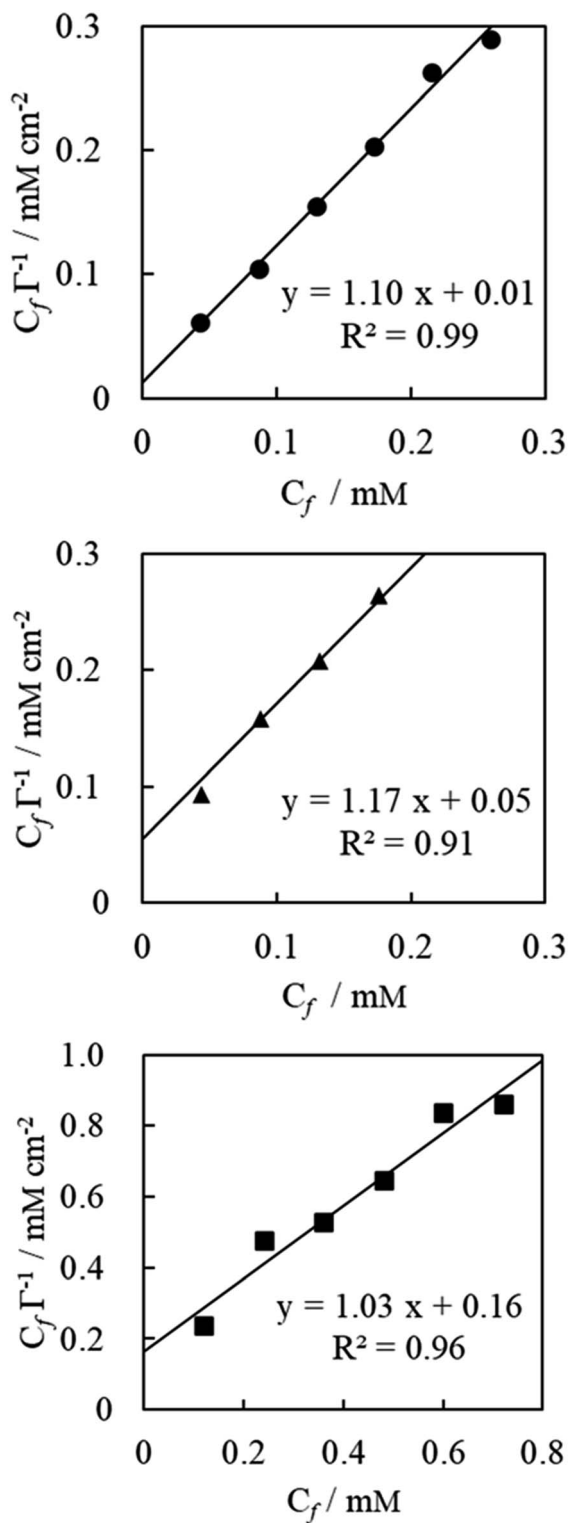
Fig. 3 Saturation curve analysis according to Hanes−Woolf plot linearity for MG (measured at 622 nm, represented by closed circles), R6G (527 nm, closed triangles), and FL (441 nm, closed squares). Concentration of dyes C_f was substituted with their preparation concentration of soaking solution. Adsorption Γ represents the reflection absorption of the evaporative dried membrane, which was washed with ultrapure water and air-dried overnight. Plain saturation curve is shown in ESI Fig. S2.†

derivatives of TPM. As adsorption on PTFE is difficult, preliminary experiments were carried out under various conditions. The evaporative dried membranes of these TPM derivatives were successfully stained because the prepared solution had a quite high concentration and was not washed out.

Fig. 2 shows the reflective spectra of the membranes. FL staining of the porous PTFE membrane at the reflectance maxima is observed at 493 nm. The wavelength of the reflection peak of the adsorbed FL matches the absorption wavelength of the FL solution.[31] Similarly, the adsorbed BTB, CBB, FC, R6G, and MG of the reflectance maxima can be observed at 428, 662, 540, 540, and 661 nm, respectively.[32–34] Because the wavelength of the reflection peak of the adsorbed dye approximately matches the absorption wavelength of the dye, the dye did not decompose during the adsorption process.

The Langmuir monolayer adsorption of the TPM derivative dyes (MG, R6G, and FL) on porous PTFE membranes was examined according to the Hanes−Woolf plot linearity. First, the Hanes−Woolf equation was derived from the double reciprocal equation of Langmuir isotherms, and then both sides were multiplied by the concentration of unbound adsorbate (dye) C_f:

$$\frac{C_f}{\Gamma} = \frac{1}{n}C_f + \frac{1}{nK} \tag{1}$$

where Γ, n, and K represent adsorption, the number of sites on the unit amount of adsorbent (membrane), and association equilibrium constant, respectively.[35] We cannot define the concentration of unbound adsorbate in the case of evaporative dried membranes; thus, C_f was provisionally used to determine the concentration of the sample dye before soaking. C_f of MG and FL were 0.04, 0.08, 0.12, 0.16, 0.20, and 0.24 mg mL^{-1}, while C_f of R6G were 0.02, 0.04, 0.06, 0.08, 0.10, and 0.12 mg mL^{-1}. The adsorption was measured for the stained membrane after washing with an integral spherical spectrophotometer.

The results are presented in Fig. 3. The vertical axis of this graph is the relative reflectance absorbance so that it can be evaluated relatively, but it cannot show the amount of adsorption in absolute value. However, the washing process resulted in desorption of excess adsorbed dyes to obtain apparent saturation curves. This indicates that the limited quantity of dyes covered the membranous interface and/or penetrated the membranous matrix during soaking and/or evaporated drying.[35,36]

Optimization of the adsorption procedure for dyes on porous PTFE

As the aqueous solution was unsuitable for adsorption onto the porous PTFE membrane, we previously adopted an evaporative drying method using an acetone solution of TPM derivatives to examine their binding onto the porous PTFE. In this study, we screened the optimum solvent for the adsorption of various dyes onto a porous PTFE membrane. The selected solvents were ultrapure water and EtOH as hydrogen donors/acceptors,
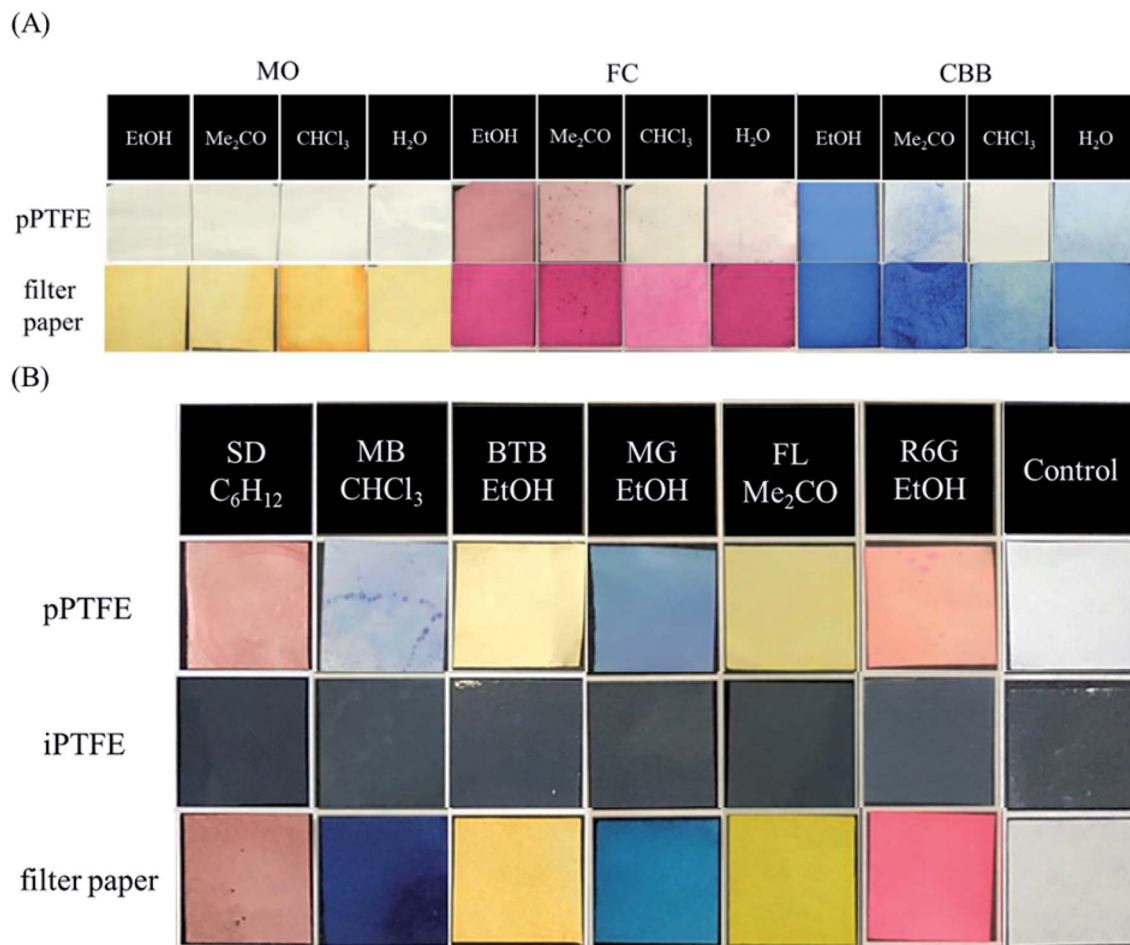
Fig. 4 Photographs of prepared PTFE membranes and filter papers (20 mm × 20 mm). (A) Porous PTFE membranes and filter papers stained with methyl orange (MO), FC, and CBB, which were dissolved in EtOH, acetone, chloroform, and water. (B) Porous PTFE membranes, intact PTFE membranes, and filter papers stained with Sudan III (SD), methylene blue (MB), BTB, MG, FL, and R6G, which were dissolved in their most appropriate solvents consequently selected. Relative reflection spectra of these porous PTFE membranes stained by dyes were measured using an integrating spherical spectrophotometer, and the results are shown in ESI Fig. S3.†

acetone as the carbonyl hydrogen acceptor, chloroform as the polarized hydrogen donor, pyridine as the aromatic hydrogen acceptor, toluene as the aromatic solvent, and cyclohexane as the aliphatic solvent.[37]

Fig. 4A shows the partial selections for the aqueous soluble anionic azo-dye, MO, and TPM derivative dyes, FC and CBB. As each dye was insoluble in nonpolar solvents, we show only the results using water, EtOH, acetone, and chloroform. Under the conditions capable of staining filter papers, the porous PTFE membranes could not be stained with MO. As described in the previous section, water-soluble dyes, such as MO, are inviolable to porous PTFE membranes. FC staining was the best in EtOH, acetone, and water, but not in chloroform. CBB staining was good in EtOH, water, and acetone, but not in chloroform. EtOH was determined to be the most appropriate solvent based on the degree of staining with FC and CBB. As shown in Fig. 4B, each dye in its suitable solvent stained the porous PTFE membrane, while it was unable to adsorb onto the intact PTFE membrane. The reflective spectra of the membranes are presented in

Fig. S3.† Reflectance peaks were observed for all dyes except MO, indicating that they adsorbed onto the porous PTFE.

SEM observations of the membranes are displayed in Fig. 5. The surface of the intact PTFE was flat and smooth. The porous PTFE membrane showed delicate structures different from the filter paper, whereas the difference in thickness of the consisting thread seemed negligible to choose between the two. The surface of the porous PTFE remained almost unchanged with or without FL/R6G/LDC adsorption, so the amount of adsorption cannot change the membrane thickness. The filter paper yielded similar results. Discrimination of the appropriate solvent would provide good adsorption of dyes with moderate hydrophobicity on activated interfaces as porous PTFE.

ATR-FTIR spectral feature of the bound dye on porous PTFE

Although we employed visible dyes because of their traceability to adsorption and desorption, most medicines are invisible, so ultraviolet/visible light optical instruments, including the
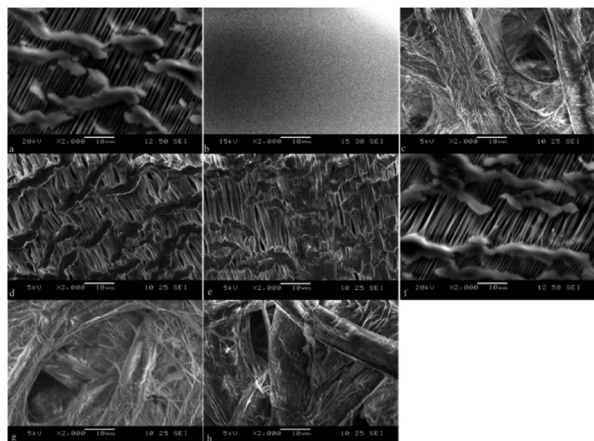
Fig. 5 SEM images of PTFE membranes and filter papers. Staining with FL and R6G did not result in any differences in observations for porous PTFE membrane and filter paper. Appropriate-solvent-stained membranes were prepared as described in the Materials and Methods section. (a) pPTFE, (b) iPTFE, (c) filter paper, (d) FL-pPTFE, (e) R6G-pPTFE, (f) LDC-pPTFE, (g) FL-filter paper, (h) R6G-filter paper.

integrating spherical spectrophotometer, are useless. The LDC adsorbed onto the porous PTFE did not exhibit reflectance peaks (Fig. S2 and S3†). Furthermore, as the melting points of the dyes were unknown due to their decomposition at high temperatures, a comparative study of the DSC thermogram could not be performed. Thus, we used a surface analysis apparatus (*i.e.*, ATR-FTIR spectrophotometer). The non-stained porous PTFE membrane exhibited potent signals at wavenumbers of 1198, 1148, 636, 555, and 502 cm^{-1} (ESI Fig. S4†). In contrast, we found that representative signals (benzyl, carbonyl, and amino groups) of the dyes adsorbed onto the porous PTFE membranes were detectable in the wavenumber range of 1800–1400 cm^{-1}.[38–40]

Fig. 6 depicts the ATR-FTIR spectra of the dyes adsorbed onto the porous PTFE membranes. These spectra were obtained after subtracting the background (intact porous PTFE) from the sample (stained porous PTFE) spectra. Although we observed no spectral signals originating from the water-soluble dyes, MO, MB, and BTB adsorbed on the porous PTFE membranes in this wavenumber range; the apparent signals of the CBB, FC, FL, MG, R6G, and SD were confirmed by ATR-FTIR spectral differences between the stained and non-stained membranes. We found signals of MO, MB, and BTB in this wavenumber range in the crystalline powder spectra. MO was unable to stain the porous PTFE membrane, as shown in Fig. 4A, whereas MB and BTB adsorbed on the membrane were stained in visible light, as shown in Fig. 4B. This indicates that the ATR-FTIR spectra of MB and BTB were lost due to adsorption on the porous PTFE membrane.

Although we detected insignificant differences in the corresponding spectra of MG and R6G adsorbed on the porous PTFE membrane from the crystalline ATR-FTIR spectra of MG and R6G, apparent spectral changes between the adsorbed dyes and their crystalline powders were observed for CBB, FC, FL, and SD. The peak at 1572 cm^{-1} for the CBB crystalline powder shifted to 1586 cm^{-1} for CBB adsorbed on the porous PTFE membrane. For FC, the crystalline peak at 1575 cm^{-1} shifted to the membranous peak at 1590 cm^{-1}. The blueshift indicates an increase in the infrared absorbed energy, which is inversely proportional to the wavelength. Hence, the blueshift occurs toward lower wavelengths. Shifts to lower wavelengths have been reported to exhibit π–π stacking and hydrophobic interactions in compounds with aromatic rings.[41] Furthermore, hydrophobic interactions of protein adsorption have been observed to shift to lower wavelengths.[42] We concluded that this blueshift indicates a hydrophobic interaction between the dyes and the porous PTFE. Meanwhile, the SD crystalline powder exhibited an isolated peak at 1501 cm^{-1}, whereas the adsorbed
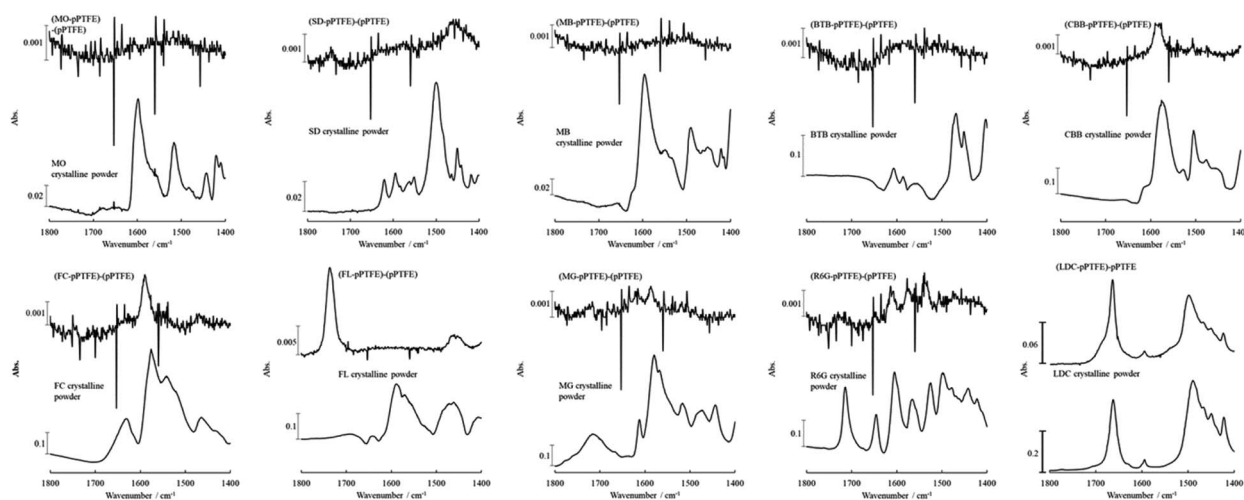

Fig. 6 ATR-FTIR spectra of dyes/LDC adsorbed on the porous PTFE membranes. Appropriate-solvent-stained membranes were prepared as described in the Materials and Methods section. Difference spectrum, indicated as (dyes/LDC-PTFE)-PTFE, were obtained after subtracting the porous PTFE from the stained porous PTFE or the LDC adsorbed porous PTFE. ATR-FTIR spectra of the porous PTFE, the stained porous PTFE, and the LDC adsorbed porous PTFE are shown in Fig. 1B and S4.†

SD showed the highest peak at 1460 cm^{-1}. We observed drastic changes in the membranous and crystalline FL spectra. The peak at 1590 cm^{-1} observed in the spectrum of FL crystalline powder was annihilated, and a sharp peak at 1738 cm^{-1} appeared on the spectral component of FL adsorbed on the porous PTFE membrane. Interestingly, the peak at 1490 cm^{-1} of the LDC crystalline powder shifted to 1499 cm^{-1} for LDC adsorbed on the porous PTFE membrane. This shift followed the same pattern as that observed for CBB and FC.

We collected multiple ATR-FTIR spectral changes and/or retention cases depending on the TPM derivatives and other adsorbates. However, we could not comprehend the simple regularity of the spectral transformations between adsorption and crystalline powders. Moreover, the apparent spectral changes between the adsorbent dyes and their crystalline powders demonstrated by CBB and FC were similar to those of LDC. LDC adsorbed on the porous PTFE membrane was an intact crystal. Mingyu *et al.* reported that TPM-derived dyes, such as R6G, are self-organized.[43] It was suggested that an endothermal signal at a temperature lower than the melting point of LDC crystalline powder on a DSC thermogram indicates that the crystals on the PTFE membrane are self-organized.[44]

Conclusions

We successfully found that TPM dyes and LDC adsorbed onto porous PTFE under specified conditions, investigated various changes caused by adsorption, and estimated the adsorption mechanism. These adsorption phenomena showed the potential to remove organic dyes in industries and remove the overdose of LDC in dentistry. The wavelengths of the reflection peaks of the adsorbed TPM dyes matched the absorption wavelengths of the dyes. Thus, the dye did not decompose during adsorption. The adsorption of the TPM derivative dyes (MG, R6G, and FL) on the porous PTFE membranes obtained apparent saturation curves. This indicates that a limited quantity of dyes covering the membranous interface penetrated the membranous matrix. The adsorption of the dyes was analyzed *via* ATR-FTIR spectroscopy to evaluate the adsorption of invisible medicines. The adsorption mechanism at the molecular level could not be determined. However, the apparent spectral changes of CBB and FC between the intact and adsorbed samples were similar to those of LDC. These results suggest a hydrophobic interaction between the dyes/LDC and porous PTFE, so flat-structured molecules are associated with adsorption onto the porous PTFE membrane due to self-organized stacking. If the positive charge of LDC can be aligned with PTFE, the arrangement of charged molecules on PTFE may lead to dissociation of a drug in response to a change in pH, indicating the possibility of new applications of PTFE. Thus, in our study, we discovered an important adsorption phenomenon for new applications of PTFE.

Author contributions

Kengo Mitsuya: investigation, visualization, writing – original draft. Satoru Goto: investigation, supervision. Yuta Otsuka: writing – review and editing. Yayoi Kawano: writing – review and editing. Takehisa Hanawa: writing – review and editing.

Conflicts of interest

There are no conflicts to declare.

Notes and references

1 S. S. Ozdemir, M. G. Buonomenna and E. Drioli, *Appl. Catal., A*, 2006, **307**, 167–183.

2 D. M. Warsinger, S. Chakraborty, E. W. Tow, M. H. Plumlee, C. Bellona, S. Loutatidou, L. Karimi, A. M. Mikelonis, A. Achilli, A. Ghassemi, L. P. Padhye, S. A. Snyder, S. Curcio, C. D. Vecitis, H. A. Arafat and J. H. Lienhard, *Prog. Polym. Sci.*, 2018, **81**, 209–237.

3 L. Nyholm, G. Nyström, A. Mihranyan and M. Strømme, *Adv. Mater.*, 2011, **23**, 3751–3769.

4 A. Thomas, P. Kuhn, J. Weber, M. M. Titirici and M. Antonietti, *Macromol. Rapid Commun.*, 2009, **30**, 221–236.

5 T. Kitamura, K. I. Kurumada, M. Tanigaki, M. Ohshima and S. I. Kanazawa, *Polym. Eng. Sci.*, 1999, **39**, 2256–2263.

6 E. Stojanovska, E. Canbay, E. S. Pampal, M. D. Calisir, O. Agma, Y. Polat, R. Simsek, N. A. Serhat Gundogdu, Y. Akgul and A. Kilic, *RSC Adv.*, 2016, **6**, 83783–83801.

7 J. Dai, X.-L. Xu, J.-H. Yang, N. Zhang, T. Huang, Y. Wang, Z.-W. Zhou and C.-L. Zhang, *RSC Adv.*, 2015, **5**, 20663–20673.

8 J. J. Bauer, B. A. Salky, I. M. Gelernt and I. Kreel, *Ann. Surg.*, 1987, **206**, 765–769.

9 J.-Y. Park, J.-H. Lee, C.-H. Kim and Y.-J. Kim, *RSC Adv.*, 2018, **8**, 34359–34369.

10 J. Imbrogno, L. Rogers, D. A. Thomas and K. F. Jensen, *Chem. Commun.*, 2018, **54**, 70–73.

11 O. A. Budnik, V. A. Sviderskii, A. F. Budnik, K. V. Berladir and P. V. Rudenko, *Chem. Petrol. Eng.*, 2016, **52**, 63–68.

12 C. W. Extrand, *J. Fluorine Chem.*, 2003, **122**, 121–124.

13 K. Ozeki, I. Nagashima, Y. Ohgoe, K. K. Hirakuri, H. Mukaibayashi and T. Masuzawa, *Appl. Surf. Sci.*, 2009, **255**, 7286–7290.

14 Y. Kawano, S. Otsu, T. Baba and T. Hanawa, *Yakugaku Zasshi*, 2017, **137**, 1409–1417.

15 E. Dhanumalayan and G. M. Joshi, *Adv. Compos. Hybrid Mater.*, 2018, **1**, 247–268.

16 S. H. Mollmann, J. T. Bukrinsky, S. Frokjaer and U. Elofsson, *J. Colloid Interface Sci.*, 2005, **286**, 28–35.

17 C. J. V. Oss, R. J. Good and M. K. Chaudhury, *J. Colloid Interface Sci.*, 1986, **111**, 378–390.

18 R. Konradi, B. Pidhatika, A. Mühlebach and M. Textor, *Langmuir*, 2008, **24**, 613–616.

19 A. C. Fröhlich, G. S. D. Reis, F. A. Pavan, É. C. Lima, E. L. Foletto and G. L. Dotto, *Environ. Sci. Pollut. Res.*, 2018, **25**, 24713–24725.

20 G. R. S. Cavalcanti, M. G. Fonseca, E. C. D. S. Filho and M. Jaber, *Colloids Surf., B*, 2019, **176**, 249–255.

21 A. Janas-Naze and P. Osica, *Int. J. Occup. Med. Environ. Health*, 2019, **32**, 333–339.

22 V. Singh, M. Thepra, S. Kirti, P. Kumar and K. Priya, *J. Oral Maxillofac. Surg.*, 2018, **76**, 2091.e1.

23 Y. Shimada, S. Goto, H. Uchiro, K. Hirota and H. Terada, *Colloids Surf., B*, 2013, **105**, 98–105.

24 R. Tateuchi, N. Sagawa, Y. Shimada and S. Goto, *J. Phys. Chem. B*, 2015, **119**, 9868–9873.

25 Y. Shimada, S. Goto, H. Uchiro, H. Hirabayashi, K. Yamaguchi, K. Hirota and H. Terada, *Colloids Surf., B*, 2013, **102**, 590–596.

26 H. Kataoka, Y. Sakaki, K. Komatsu, Y. Shimada and S. Goto, *J. Pharm. Sci.*, 2017, **106**, 3016–3021.

27 H. Chatani, S. Goto, H. Kataoka, M. Fujita, Y. Otsuka, Y. Shimada and H. Terada, *Chem. Phys.*, 2019, **525**, 110415.

28 J. Fu, Q. Xin, X. Wu, Z. Chen, Y. Yan, S. Liu, M. Wang and Q. Xu, *J. Colloid Interface Sci.*, 2016, **461**, 292–304.

29 S. Kurada, G. W. Rankin and K. Sridhar, *Opt. Lasers Eng.*, 1994, **20**, 177–192.

30 S. Shimizu, A. Hirai, Y. Li, Y. Shimada, S. Goto and T. Iwase, *Yakuzaigaku*, 2018, **78**, 101–108.

31 R. Sjöback, J. Nygren and M. Kubista, *Spectrochim. Acta, Part A*, 1995, **51**, L7–L21.

32 E. Klotz, R. Doyle, E. Gross and B. Mattson, *J. Chem. Educ.*, 2011, **88**, 637–639.

33 C. Würth, M. G. González, R. Niessner, U. Panne, C. Haisch and U. R. Genger, *Talanta*, 2012, **90**, 30–37.

34 X. Zhang, S. Zheng, Z. Lin and S. Tan, *J. Appl. Polym. Sci.*, 2012, **123**, 2250–2256.

35 M. Dixon and E. C. Webb, *Enzyme kinetics in enzymes*, Academic press, New York San Francisco, 3rd edn, 1979.

36 J. G. Lopez, E. V. Piletska, M. J. Whitcombe, J. Czulak and S. A. Piletsky, *Chem. Commun.*, 2019, **55**, 2664–2667.

37 I. M. Smallwood, *Handbook of organic solvent properties*, Halsted Press, New York, 1996.

38 C. Y. Liang and S. Krimm, *J. Chem. Phys.*, 1956, **25**, 563–571.

39 D. Q. Balbas, S. Prati, G. Sciutto, E. Catelli and R. Mazzeo, *New J. Chem.*, 2019, **43**, 9411–9419.

40 L. C. Lee, M. R. Othman, H. Pua and A. A. Ishak, *Malay. J. Forensic Sci.*, 2012, **3**, 5–10.

41 T. R. B. Ramakrishna, M. Mathesh, Z. Liu, C. Zhang, A. Du, J. Liu, C. J. Barrow, M. Chen, M. J. Biggs and W. Yang, *Langmuir*, 2020, **36**, 13575–13582.

42 C. E. Giacomelli, M. G. E. G. Bremer and W. Norde, *J. Colloid Interface Sci.*, 1999, **220**, 13–23.

43 M. Chapman, M. Mullen, E. Novoa-Ortega, M. Alhasani, J. F. Elman and W. B. Euler, *J. Phys. Chem. C*, 2016, **120**, 8289–8297.

44 B. Hachuła, A. Polasz, M. Książek, J. Kusz, O. Starczewska and W. Pisarski, *Spectrochim. Acta, Part A*, 2017, **183**, 378–386.